Published by :
http://www.ijert.org

International Journal of Engineering Research & Technology (IJERT)
ISSN: 2278-0181
Vol. 9 Issue 03, March-2020

Effect of Synthesis Route on Photocatalytic Properties of 10% Ti Doped $Bifeo_3$ Nanoparticles

Nafiza Anjum
Dept of Mechanical Engineering, SUST
Sylhet, Bangladesh

Syeda Noor E Lamia
Dept of Mechanical Engineering,
University of Delaware Delaware, USA

Md. Yeashir Arafat
Dept of Mechanical Engineering, BUET
Dhaka, Bangladesh

Abdullah Al Noman
Dept of Mechanical Engineering, BUET
Dhaka, Bangladesh

***Abstract*— $BiFeO_3$ (BFO) is drawing significant attention due to its growing potential as a multiferroic ceramic and applicability as photocatalyst. Our previous research showed that, Ti doping with BFO results in an increased ability of the sample for photocatalytic H_2 fuel generation. This article is aimed at studying the photocatalytic properties of 10% Ti doped $BiFeO_3$ ceramic and investigate the effect of synthesis route on the properties. Conventional sol-gel technique were followed in this experiment to prepare $BiFe_{0.9}Ti_{0.1}O_3$ (BFTO) nanoparticles, which is a bottom-up synthesis process. 2-methoxy ethanol were used as solvent and to prevent agglomeration, citric acid was used as a capping agent. The Energy Dispersion Spectroscopy (EDS) analysis confirmed the homogeneous substitution of Ti in $BiFeO_3$ nanoparticles. From the X-ray Diffractometer (XRD) patterns, structural modifications were investigated and compared. FESEM results showed that finer grade particles were synthesized from sol-gel method. The band gap energy of the selected samples was estimated from their Diffused Reflectance Spectra (DRS) graphs by applying Kubelka-Munk (KM) function. The absorption spectra confirmed that, the prepared sample can absorb light with wavelength from UV to visible region. It also exhibited higher band gap energy compared to the samples prepared from other top-down process.**

Keywords—Multiferroic; photocatalysis; perovskite; Bismuth Ferrite; Titanium doping; XRD; UV-Vis Spectroscopy

I. INTRODUCTION

In spite of having some inherited drawbacks, like, wide band gap, instability, photocorrosion, and the photogenerated charge carrier recombination etc, photoelectrocatalysts have recently obtained notable attentions worldwide. TiO_2, WO_3, Fe_2O_3, $BiVO_4$ etc photoelectrocatalysts are recently being investigated [1, 2]. Among the numerous classes of materials, perovskites-based photocatalysts have distinct photophysical properties and offer unique advantages. Perovskites have the general formula as ABO_3, where the A site and B site is occupied by the larger cation and the smaller cation, respectively. The perovskite has octahedral crystal structure where the eight corners are occupied by BO_6 atoms. 12 oxygen coordinated A cations are located in between the eight BO_6 octahedra [3, 4]. However, the phenomena of tilting of the octahedra occurs depending on the electromagnetive properties of the A and B cations and their ionic radii. This tilting might result in lower symmetry structures and varied electronic and optical properties. Different properties like, the band structure, electron and hole transportation, photoluminescence, and dielectric behavior [3, 2, 4] is affected by the degree of tilting. In photocatalysis, there are several reasons for the perovskite structures being significantly advantageous while comparing with the corresponding binary oxides. Firstly, perovskites have the potentiality to offer favorable band edge potentials allowing various photoinduced reactions. Secondly, A and B site cations can be engineered in the lattice allowing a wide scope to modify the band structure and other photophysical properties [4]. Thirdly, combining the effects of ferroelectricity with the photocatalytic effect gives rise to the photocatalytic activity, which is possible in perovskites. The enhancement of electron-hole separation and photocatalytic activity can be triggered utilizing the ferroelectric properties of BFO. Although, the ferroelectric properties of BFO has been studied, its other properties like, moderate band gap (2.2 eV), appropriate band edge positions, stability and nontoxicity indicate its suitability as a photoelectrocatalyst for water oxidation.

$BiFeO_3$ is, however, difficult to put in application due to its having low resistivity and the synthesis process of the pure phase being intrinsic and difficult [1]. Some improvements in the methodology of synthesis has been studied to reduce formation of impurity phases [5, 6, 3]. Recent researches are targeting to modify the magnetic, electric and optical properties of BFO by doping it with different transition metal ions, paramagnetic rare earth metal ions or non-magnetic alkaline earth metal ions. Bi^{3+} ion of BFO when substituted with rare-earth elements, such as La^{3+}, Nd^{3+} or Sm^{3+} results in remarkable improvement of the ferroelectric and ferromagnetic properties [6, 2, 4, 7]. Previous investigation demonstrate that Gd-doped $BiFeO_3$ shows enhanced photocatalytic degradation for Rhodamine B (RhB) [8]. It is also shown that Ca doped BFO improves the photocatalytic degradation of Congo Red dye [9]. Yan-Nan Feng and Huan-Chun Wang et al also found a similar results from their studies [10]. Ben Wang et al showed that, small amount of Sr^{2+} doping to BFO can create phase transition from the rhombohedral distorted perovskite to the cubic structure. The

International Journal of Engineering Research & Technology (IJERT)
ISSN: 2278-0181
Vol. 9 Issue 03, March-2020

substitution of heterovalent Sr^{2+} ions in BFO nanoparticles leads to better ferromagnetic property [11].
However, not much studies were done on the effect of transitional metal ion such as Ti doping on BFO. Again, there are very few works on methodological comparison to establish an effective route to fabricate pure phase nanoparticles with improved properties. The selection of Ti as a dopant ion is based on the facts that-

- The ionic radius of Ti (0.605 A˚) is quite similar with that of Fe ion (0.645 A˚), which is conducive to the replacement [12].
- Ti^{+} is highly aliovalent compared to the other cations Bi and Fe and [12]
- Ti atoms have partially filled 3d orbitals which can improve the position of the valence band [13] (VB) and change the band gap structures of semiconductors.
- Intriguing properties are reported for other Titanium-doped nanomaterial [12, 13].

A promising way of enhancing the multiferroic properties of $BiFeO_3$ is to prepare the nanoparticles with particle sizes smaller than 62 nm which is actually the size of the spiral modulated spin structure of BiFeO3 [13]. Notably, synthesis of $BiFeO_3$ multiferroic nanoparticles with improved ferromagnetic, ferroelectric and photocatalytic properties with a particle size of the order of or smaller than 62 nm is still a challenge to the research community. Recently, a physical technique was developed in Nanotechnology Research Laboratory, Department of Physics, BUET to produce high quality BiFeO3 nanoparticles directly from their bulk powder materials using ultrasonic energy [8]. In the present investigation, nanoparticles of BFTO were fabricated following the conventional Sol-gel methodology to observe the suitability of these two comparable routs. The structural, morphological and optical properties were investigated for both bulk polycrystalline materials and their corresponding nanoparticles. Investigation of the surface morphology and the crystal structure of the samples were done by using Field Emission Scanning Electron Microscope (FESEM) and X-Ray Diffraction (XRD) techniques, respectively. Optical properties such as absorbance, reflactance and band-gap energy were investigated using UV-vis spectrometer.

II. METHODOLOGY

A. Sample Preparation

The calculated amounts of $Bi(NO_3)_3.5H_2O$ and $Fe(NO_3)_3.9H_2O$ were taken in two beakers separately. To dissolve these, ~70 mL of 2-methoxy ethanol (each) was used as the solvent. In another beaker, ~50 mL of 2-methoxy ethanol was poured, and Ti Butoxide was introduced in it with the help of a pipette according to the calculation. Here to mention that Ti Butoxide reacts readily with the moisture in air, and forms a solid. To avoid this, the process needs to be fast. Citric acid was also dissolved in 2-methoxy ethanol. It acts as a capping agent.
Sol-gel being a bottom up process, the particles grow larger from atomic scale. When these are small enough, their surface energy is much higher. To reach an equilibrium of energy, the particles tend to agglomerate on the surface. This may reduce the photocatalytic properties of the particles. Citric acid hinders this process. Three separate solutions were then mixed together to form the 'sol' and stirred by a magnetic stirrer. The temperature of the solution was kept at 100°-110°C to evaporate. The temperature of the solution was not allowed to rise above 110°C, as 2-methoxy ethanol boils at ~120°C. After ~8 h of continuous stirring, the solution gained the 'gel' structure. The gel was then dried to powders, taken in a crucible for drying, and put in the oven. The temperature was set to 80°C for 24 h. To get the nanoparticles the dried the material was calcined at 650°C for 1 h. Ramping rate of the furnace was 20°C/min. The nominal composition of $BiFe_{0.9}Ti_{0.1}O_3$ (BFTO) bulk polycrystalline materials were also synthesized by a conventional solid state reaction technique and by using ultrasonication technique corresponding nanoparticles were produced directly from their bulk powder materials.

B. Characterization

To observe the crystal structure of the bulk, the pellets were g round into fine powders while the nanoparticles needed no additional measure. The structural properties and phases present in the crystalline samples were determined from the XRD patterns given by the X-Ray Diffractometer (Bruker D8, Cu-Kα1 radiation, λ = 1.540598 Å) in the range 2θ = 20°-80°. To study the surface morphology and chemical homogeneity of the samples, Field Emission Scanning Electron Microscope with Energy Dispersive X-Ray Spectroscopy (EDS) (FESEM, model: JEOL JSM 7600F) was used. The UV-visible absorbance spectra of the samples (range: 200-800 n m) were recorded using a UV-vis spectrophotometer (UV-2600, SHIMADZU) where BaSO4 was used as the reference material.

III. RESULT AND DISCUSSION

A. Structural Analysis

Successful Ti doping has been confirmed by EDS elemental analysis. EDS (Energy-dispersive X-ray spectroscopy) analysis were done for three different positions of the prepared sample and it is confirmed that, O, Ti, Fe and Bi elements are homogenously present throughout the prepared BFTO ceramic nanoparticle. As seen from EDS result (table 1), the actual Ti doping contents in the BFTO bulk sample was detected to be 3.37%, which is very close to the theoretical value. From the EDS spectra, it is observed that carbon content in the sample is very small. Calcination process in air removed almost all of the organic components of the gel which eventually resulted in low carbon content. From fig. 1 a common peak for platinum can be observed in the EDS spectra which can be attributed to the platinum coating of the particles prior to performing the spectroscopic analysis.

TABLE I. ELEMENTAL MASS PERCENTAGE

Samples	Elements	Mass %
BFTO nanoparticle prepared by sol-gel technique	O	2.65
	Ti	3.37
	Fe	20.98
	Bi	73.00

International Journal of Engineering Research & Technology (IJERT)
ISSN: 2278-0181
Vol. 9 Issue 03, March-2020

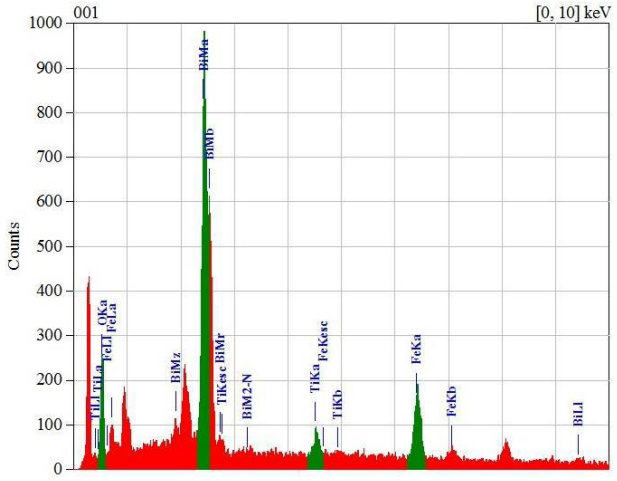

Fig. 1. EDS image of BFTO nanoparticles prepared from sol-gel method

The structural properties of $BiFe_{0.9}Ti_{0.1}O_3$ ceramics and their corresponding nanoparticles were analyzed with powder X-Ray Diffraction (XRD) method. Ti doping reduces the presence of secondary phases as has been evidenced in our previous work [14]. Main reason behind the impurities are oxygen vacancies, volatility of Bismuth and transition of Fe^{2+} to Fe^{3+}. However, the mechanism leading to the formation of those secondary phases is still unknown. The size of the particle can also be assumed from Fig. 2. Scherrer equation helps to understand this:

$$\tau = \frac{\lambda\kappa}{\Delta(2\theta)\cos\theta} \qquad (1)$$

Where,
τ = mean size of the ordered (crystalline) domains, which may be smaller or equal to the grain size;
κ = a dimensionless shape factor, with a value close to unity;
λ = X-ray wavelength;
θ = Bragg angle;
$\Delta 2\theta$ = line broadening at half the maximum intensity

So an increase in $\Delta 2\theta$ will decrease τ, so the size of the particles decreases. The nanopartilces obtained from sol-gel method shows better structure than the ultrasonication nanoparticles or the bulk (solid-state); particles are smaller with less irregularities. Also the splitting peaks are tending to merge more smoothly in the sol-gel sample.
The smaller particle size of sol-gel sample is also confirmed from FESEM (Field Emission Scanning Electron Microscope) images. From the histogram (fig. 3-b), it is evident that the grain size distribution is pretty homogeneous and the average grain size of nanoparticles has reduced to 70nm. While we observed in our previous work that the average grain size for BFTO nanoparticles prepared from ultrasonication method was 90nm [14].

It has been previously observed that Ti doping increases the porosity in surface morphology of BFTO nanoparticles. Fig. 3-a also confirms porosity which might be attributed to the inherited higher oxygen vacancies of this sample.

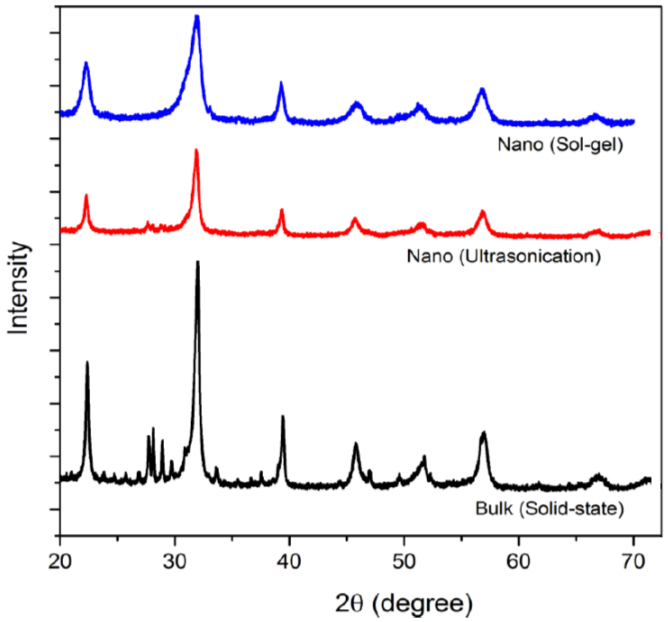

Fig. 2. XRD patterns of BFTO samples

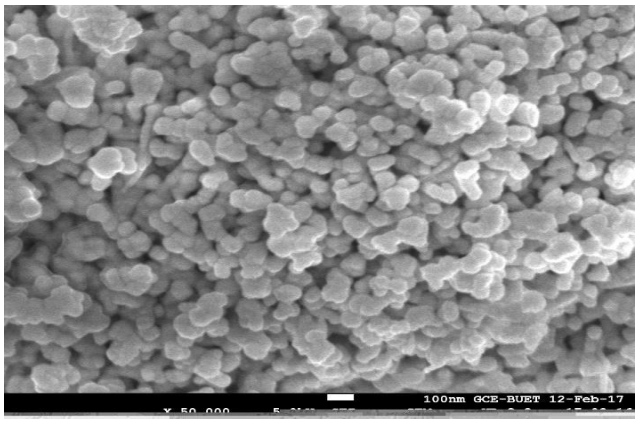

(a)

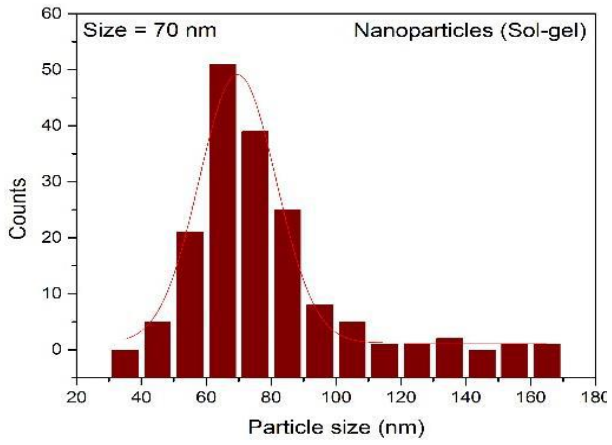

(b)

Fig. 3. (a) FESEM image of BFTO nanoparticles derived from sol-gel method under 5000 magnification. (b) particle size distribution in histogram

International Journal of Engineering Research & Technology (IJERT)
ISSN: 2278-0181
Vol. 9 Issue 03, March-2020

B. Optical Properties

The absorbance spectra of the selected samples were investigated with an aim to probing their optical properties. 10% Ti doped nanoparticles prepared by sol-gel technique shows absorption edges at 640 nm which is, although less than that for undoped bulk BFO material, higher than any other BFTO bulk and nanoparticles prepared by solid state route and ultrasonication method [14]. This evidently indicates blue-shift from its bulk sample. The blueshift may be due to the bandgap energy modification due to ultra-fine nanosized particles. However the absorption edge value shows that tested sample can absorb light with wavelength from UV to visible range.

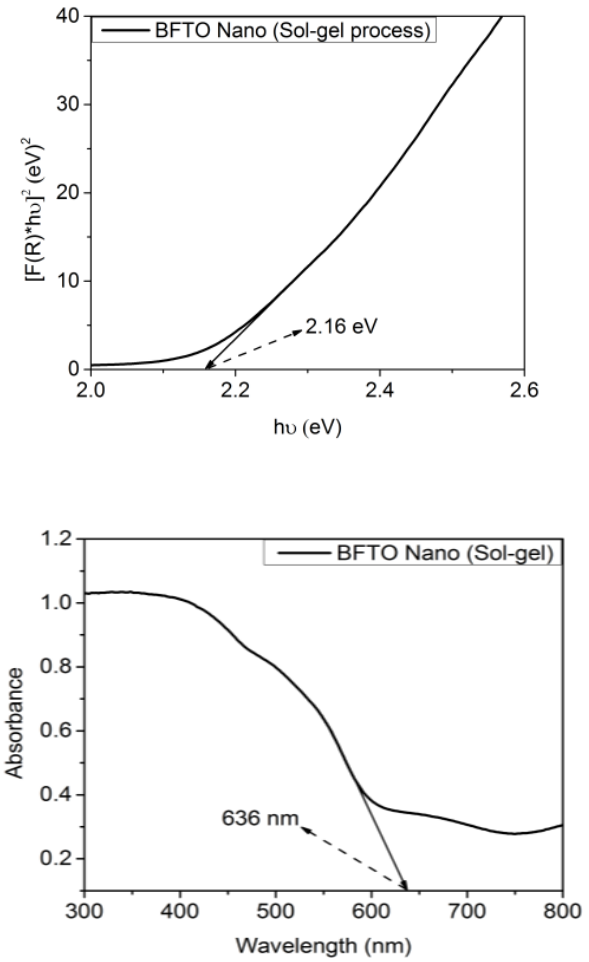

(b)

Fig. 4. (a) Diffuse spectra and (b) absorbance reflectance spectra of BFTO samples.

The Diffuse Reflectance Spectra (DRS) were performed to investigate the major transitions and to estimate the band gap energy of the synthesized selected sample. The direct band gap energies of the samples were estimated from their DRS graphs by applying Kubelka-Munk function for direct transition, where F(R) is defined as-

$$F(R) = \frac{1-R^2}{2R} \qquad (2)$$

Where, R= Reflectance.

Our previous work showed that, Ti doping caused to reduce band gap energy from 2.45 eV and 2.58 eV to 2.28 and 2.29 respectively for BFTO bulk and BFTO nanoparticle samples prepared by ultrasonication. The BFTO nanoparticles prepared by sol-gel method shows even smaller band-gap energy which is ~2.16 eV in magnitude. This decrease in band-gap energy may have happened due to the ultra-reduced size of nanoparticles as observed from the SEM patterns. The reduction in size may have affected the crystal structure [15]. Structural distortions essentially alter the bond angle in the system. In this perspective, the band gap increment found in the case of 10% Ti-doped BFO nanoparticles prepared by sol-gel method could be attributed to the lattice distortion owing to the alteration in the rotation of FeO_6 octahedra in the unit cells. Such modifications might also influence the band edge positions that lead to an increase or decrease in the band gap energy of the synthesized materials [10]. A Lower band gap energy indicates higher charge separation hence accelerate photocatalysis.

IV. CONCLUSION

10% Ti doped BFO nanoparticles were prepared using conventional sol-gel method. Comparative investigation on structural, morphological and optical properties were performed between this sample and other BFTO bulk and nanoparticles prepared from solid state and ultrasonication methods respectively. Sol-gel method produces finer grade nanoparticles which contributes to blue shift of band gap energy of the sample. Synthesized BFTO samples absorb UV ray from visible range. It also exhibits generation of less impurity phases. Due to check in formation of oxygen vacancy, Ti doping in BFO by sol-gel method is presented as more effective synthesis route. All the properties indicate its high potentiality as photocatalysis for solar H_2 fuel generation.

ACKNOWLEDGMENT

This research was performed in Nanotechnology Research Laboratory, Department of Physics, BUET, Dhaka. XRD and SEM investigations were done in Department of Glass and Ceramic Engineering, BUET.

REFERENCES

[1] Bickley, R. I., Vishwanathan, V., “Photocatalytically induced fixation of molecular nitrogen by near UV radiation", Nature, 280, 306, 1979.
[2] Guo, C., Wu, X., Yan, M., Dong, Q., Yin, S., Sato, T., Liu, S., “The visiblelight driven photocatalytic destruction of NOx using mesoporous TiO2 spheres synthesized via a ‘water-controlled release process’ ", Nanoscale, 5, 8184, 2013.
[3] Ahmed, S., Rasul, M. G., Martens, W., Brown, R., Hashib, M .A., “Advances in Heterogeneous Photocatalytic Degradation of Phenols and Dyes in Wastewater: A Review. Water Air Soil Pollut", 215, 329, 2011.
[4] Zhao, J. and Yang, X., “Photocatalytic oxidation for indoor air purification: A literature review", Build. Environ., 38, 645, 2003.
[5] Dalrymple, O. K., Stefanakos, E., Trotz, M. A., Goswami, D. Y., “A review of the mechanisms and modeling of photocatalytic disinfection", Appl. Catal. B, 98, 27, 2010.
[6] Konstantinou, I. K., Albanis, T. A., “TiO2-assisted photocatalytic degradation of azo dyes in aqueous solution: Kinetic and mechanistic investigations: A review", Appl. Catal. B, 49, 1, 2004.

International Journal of Engineering Research & Technology (IJERT)
ISSN: 2278-0181
Vol. 9 Issue 03, March-2020

[7] Gao, F., Chen, X. Y., Yin, K. B., Dong, S., Ren, Z. F., Yuan, F., Yu, T., Zou, Z. G. and Liu, J. M., "Visible-Light Photocatalytic Properties of Weak Magnetic BiFeO3 Nanoparticles", Adv. Mater., 19, 2889, 2007.

[8] Basith, M. A., Ngo, D.-T., Quader, A., Rahman, M. A., Sinha, B. L., Bashir Ahmmad, Fumihiko Hirose and Molhave, K., "Simple top-down preparation of magnetic Bi0:9Gd0:1Fe1−xTixO3 nanoparticles by ultrasonication of multiferroic bulk material", Nanoscale, 6, 14336, 2014.

[9] Tan, Y. N., Wong, C. L., Mohamed, A. R., \An Overview on the Photocatalytic Activity of Nano-Doped-TiO2 in the Degradation of Organic Pollutants", ISRN Mat. Sci., 2011, 18, 2011.

[10] Yan-Nan Feng, Huan-Chun Wang, Yi-Dong Luo, Yang Shen, and Yuan-Hua Lin, Journal of Applied Physics 113, 146101 (2016)

[11] Ben Wang, Shumei Wang , Lixiu Gong, Zhufa Zhou, Ceramics International, Volume 38, Issue 8,

[12] Bhalla, A. S., Guo, R. and Roy, R., "The perovskite structure-a review of its role in ceramic science and technology", Mat. Res. Innov., 4, 3, 2000.

[13] Zhang, W. F., Tang, J. and Ye, J., "Photoluminescence and photocatalytic properties of SrSnO3 perovskite", Chem. Phys. Lett., 418, 174, 2006.

[14] Nafiza Anjum, Syeda Noor E. Lamia, Md. Yeashir Arafat, Monon Mahboob and M. A. Basith, "Photocatalytic Properties of Ti-Doped BiFeO3 Bulk and Nanoparticles for Solar Hydrogen Fuel Generation", AIP Conference Proceedings 1980, 060004 (2018)

[15] Ahmmad, B., Islam, M. Z., Billah, A., and Basith, M. A., \Large difference between the magnetic properties of Ba and Ti co-doped BiFeO3 bulk materials and their corresponding nanoparticles prepared by ultrasonication", J. Phys. D: Appl. Phys., 2016.